

RSC Advances



This is an *Accepted Manuscript*, which has been through the Royal Society of Chemistry peer review process and has been accepted for publication.

Accepted Manuscripts are published online shortly after acceptance, before technical editing, formatting and proof reading. Using this free service, authors can make their results available to the community, in citable form, before we publish the edited article. This *Accepted Manuscript* will be replaced by the edited, formatted and paginated article as soon as this is available.

You can find more information about *Accepted Manuscripts* in the [Information for Authors](#).

Please note that technical editing may introduce minor changes to the text and/or graphics, which may alter content. The journal's standard [Terms & Conditions](#) and the [Ethical guidelines](#) still apply. In no event shall the Royal Society of Chemistry be held responsible for any errors or omissions in this *Accepted Manuscript* or any consequences arising from the use of any information it contains.

Corrosion control in oil wells tubing steel during matrix acidizing operations

M. A. Migahed, E.G. Zaki, M. M. Shaban*

Egyptian petroleum Research Institute, Nasr city, Cairo (11727), Egypt

Abstract

Dodecyl dimethyl benzyl ammonium bromide (DDBAB) was used as corrosion inhibitor for carbon steel pipeline in 8% sulfamic acid solution during matrix acidizing operations. The inhibition efficiency (η %) has been studied by chemical (weight loss) and electrochemical (electrochemical impedance spectroscopy (EIS), potentiodynamic polarization) techniques. The surface active properties of this surfactant were calculated from surface tension measurements. Results obtained from both chemical and electrochemical techniques reveal that this compound is a very good corrosion inhibitor even at low concentrations and the maximum inhibition efficiency (93.7) was obtained at 150 ppm of DDBAB. Polarization curves showed that the corrosion current density was decreased by increasing the inhibitor concentration until critical micelle concentration (CMC) is reached. The Tafel polarization data indicate that the selected compound act as mixed type inhibitor. The slopes of the cathodic and anodic Tafel lines (β_c and β_a) are approximately constant and independent of the inhibitor concentration. Analysis of the impedance spectra indicates that the charge transfer process mainly controls the corrosion process of carbon steel in 8 % sulfamic acid solution both in the absence and presence of the inhibitor. The data obtained from EIS technique were analyzed to model the corrosion inhibition process through equivalent circuit (EC). The effect of molecular structure on the inhibition efficiency was investigated by quantum chemical calculations. The adsorption of this compound on the surface carbon steel follows the Langmuir adsorption isotherm. From the adsorption isotherm, the values of adsorption equilibrium constant (K_{ads}) and free energy of adsorption were calculated and discussed. The relatively high value of (K_{ads}) reveals a strong interaction between the inhibitor molecules and the carbon steel surface. The strong adsorption ability of this compound can be attributed to the presence of adsorption center of nitrogen as well as π donor moieties. Finally, EDX and SEM surface analysis tools were used to examine the nature of the formed protective film on carbon steel alloy.

Keywords:

Corrosion inhibitor, Cationic surfactant, Carbon steel, 8% sulfamic acid solution, EIS, Polarization, SEM, EDX , Adsorption process, Surface tension (γ) and critical micelle concentration (CMC)

*Corresponding author. Tel.: +20 1060229075.

E-mail address: mahmoud_shaban26@yahoo.com (M. M. Shaban).

1. Introduction

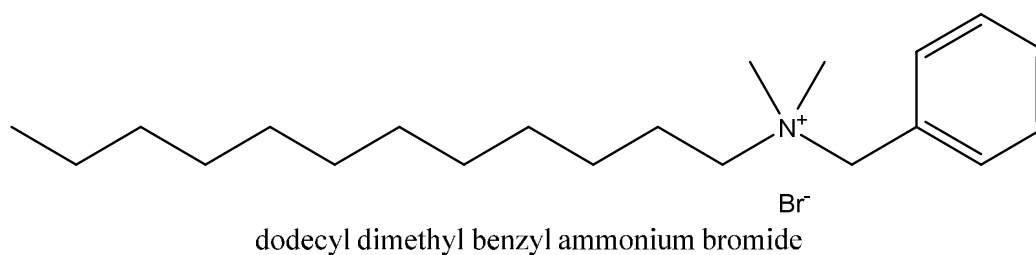
It is well known that the presence of sediments and mud solids retard the permeability of crude oil or natural gas through the wells and thus affecting the production rate. So that the main object of this job is to increase well productivity through stimulating flow of hydrocarbons as indicated in **Fig. 1 [1]**. There are different acids used to perform an acid job. A common type of acid employed on wells to stimulate production is sulfamic acid solution ($\text{H}_4\text{N}_2\text{SO}_2$), which is useful in removing carbonate reservoirs or limestone and dolomite from the rock **[2-4]**. Using of 8 % sulfamic acid solution is preferable to use in comparison to mineral acids for its intrinsic safety and having desirable water descaling properties, low volatility, and low toxicity. In order to protect the integrity of the completed well, an effective type of corrosion inhibitor must be injected to the well to prohibit the acid from breaking down the steel casing in the well **[5]**. Carbon steel, the most widely used engineering material, corrode in many circumstances, especially in some industrial processes, such as acid cleaning, acid de-scaling and oil well acidizing **[6-8]**. Excellent corrosion inhibitors are considered to be such organic compounds which not only provide offer electrons to unoccupied d orbitals of carbon steel surface to form coordinate covalent bond, but also can accept the free electrons from the surface of carbon steel as well, by using their antibond orbital to form feedback bonds in turn **[9]**. Quantum chemistry calculations have been widely used to study the reaction mechanisms and to interpret the experimental results as well as to solve chemical ambiguities. Recently, some corrosion publications have contained large quantum chemical calculations **[10, 11]**. Such calculations are performed here to throw more light on the adsorption mode of the inhibitor. Actually, few papers in the literature deal with the subject of corrosion and corrosion inhibition of carbon steel in 8% solution of sulfamic acid, which is the real concentration in matrix acidization of old oil wells **[12-14]**. For this purpose, this work is aimed to study the performance of a new type of cationic surfactant namely, dodecyl dimethyl benzyl ammonium bromide (DDBAB), as corrosion inhibitor for X-70 type carbon steel in 8% sulfamic acid solution during matrix acidizing operations. Also the work is extended to present a theoretical study on the electronic and molecular structure of dodecyl dimethyl benzyl ammonium bromide obtained through quantum chemistry calculations carried out by the Materials Studio 7.0 program. In addition, we will attempt to find the relationship between the molecular structure of

this inhibitor and their inhibition efficiency for the inhibitor as calculated from chemical and electrochemical techniques.

Experimental

2.1. Chemicals

Commercially available dodecyl dimethyl benzyl ammonium bromide (DDBAB) was purchased from the El Gomhoria Trade Pharmaceuticals and Chemicals Company, Cairo, Egypt. This compound was used without any further purification. The chemical structure of the compound is as follows.



2.2. Preparation of aggressive Solution

The aggressive solution (8 % sulfamic acid) was prepared by dilution of sulfamic acid with distilled water. The concentration range of the dodecyl dimethyl benzyl ammonium bromide (DDBAB) cationic surfactant was from 50 to 150 ppm used for corrosion measurements. All solutions were prepared using distilled water.

2.3. Procedure used for corrosion measurements

2.3.1. Gravimetric measurements

Gravimetric measurements were performed with API X 70 – type carbon steel specimens having a composition of (wt %): 0.12 C, 0.55 Si, 1.60 Mn, 0.036 P, 0.034 S and the remainder is Fe. The used coupons in gravimetric measurements have diameters (2.5 cm x 2.0 cm x 0.2 cm). The carbon steel specimens were abraded with a series of emery paper (grade 320, 500, 800, 1000, 1200 and 2500) and then washed with bi-distilled water and acetone [15]. After weighing accurately, the specimens were immersed in 250 solution of 8 % sulfamic acid without and with the tested inhibitor (DDBAB) at different concentrations (30, 60, 90, 120 and 150 ppm) for 28 h at 25 °C. All the aggressive acid solutions were closed. After 28 h, the specimens were taken out, washed, dried and weighed accurately. The test was performed for three specimens and the weight was the average of the three specimens

2.3.2. Electrochemical measurements

Electrochemical experiments were carried out using a Voltalab 80 Potentiostat PGZ 402 in a conventional electrolytic cell with three-electrode arrangement: saturated calomel electrode (SCE) as a reference electrode, platinum electrode used as an auxiliary electrode and the working electrode (WE) had the form of a rod of carbon steel embedded in an epoxy resin of polytetrafluoroethylene (PTFE) [16]. Prior to each experiment, surface of the working electrode was mechanically polished with successive grades of emery papers down to 2500 grade of emery paper, rinsed with bi-distilled water and acetone, respectively, and then dried quickly [17]. The electrode potential was allowed to stabilize 60 min before starting the measurements. The exposed electrode area to the corrosive solution was 0.7 cm^2 . All experiments were carried out at 25°C .

Potentiodynamic polarization curves were obtained by changing the electrode potential automatically (from - 750 to - 350 mV vs. SCE) at open circuit potential with scan rate of 2 mV s^{-1} .

EIS measurements were carried out in the frequency range between 100 kHz and 50 mHz with amplitude of 10 mV peak-to-peak using AC signals at open circuit potential. EIS diagrams are given in both Nyquist and Bode plots [18]. Each experiment was repeated three times to ensure reproducibility. Measurements were performed with a Voltalab 80 Potentiostat PGZ 402 and controlled by Tacussel corrosion analysis software model (Voltmaster 4).

2.4. Surface morphology studies

Scanning electron microscope (SEM) studies and energy dispersive X-ray analysis (EDX) were performed to observe the morphology and discuss quantitative analysis of elements on the surface morphologies of the corroded specimens using JEOL JSM-5410 before and after exposure to 8% of sulfamic acid for 28 hrs in the absence and presence of 150 ppm of the DDBAB inhibitor at $25 \pm 1^\circ\text{C}$. The energy of the acceleration beam employed was 30 kV [19].

2.5. Theoretical Calculations.

Quantum chemical calculations can provide insight into the inhibitor system and elucidate the adsorption process at a molecular level [20–23]. The quantum chemical calculations were performed using DMOL³ module [24] of the Materials Studio 7.0 software (Accelrys Inc.) [25], which is designed for the realization of large scale density functional theory (DFT) calculations. DFT semi-core pseudopods calculations

(dspp) were performed with the double numerical basis sets plus polarization functional (DNP). The DNP basis sets are of comparable quality to 6–31G GAUSSIAN basis sets [26]. Delley et al. showed that the DNP basis sets are more accurate than GAUSSIAN basis sets of the same size [27]. The RPBE functional [28] is so far the best exchange–correlation functional [29], based on the generalized gradient approximation (GGA), is employed to take account of the exchange and correlation effects of electrons. The geometric optimization is performed without any symmetry restriction. The following quantum chemical indices were considered: the energy of the highest occupied molecular orbital (E_{HOMO}), the energy of the lowest unoccupied molecular orbital (E_{LUMO}), Energy gap (ΔE) = $E_{\text{LUMO}} - E_{\text{HOMO}}$, the dipole moment (μ), Electronegativity(X), Chemical potential (π) = $-X$, Hardness (η), Softness (σ) = $1/\eta$ and No. of electron transfer (ΔN). Frontier molecular orbitals (HOMO and LUMO) could be used to predict the adsorption centers of the inhibitor molecule. For the simplest transfer of electrons, adsorption should occur at the part of the molecule where the softness, σ , which is a local property, has the highest value.

2.6. Surface Tension Measurements

Freshly prepared aqueous dodecyl dimethyl benzyl ammonium bromide (DDBAB) cationic surfactant solutions with concentration range of 0.01–0.0000003ML⁻¹ were poured into a clean 25mL Teflon holder and allowed to equilibrate for 2 hrs. The platinum ring was adjusted at the air-water interface of the surfactant solution, then the reading was recorded when the ring detached itself from the solution surface. Apparent surface tension values [30] were measured a minimum of three times and the recorded values were taken as the average of these values at 25 °C. The platinum ring was then removed after each reading, washed with diluted HCl followed by distilled water.

3. Results and Discussion

3.1. Gravimetric measurements

Fig. 2 shows the weight loss–time curves of carbon steel immersed in 8 % sulfamic acid solution in the absence (blank) and presence of various concentrations of the inhibitor (DDBAB). It is evident from the figure that, the curves obtained in the presence of the inhibitor fall significantly below that obtained for blank. Also, it is clear that the weight loss of the metal decreases with increasing the inhibitor concentration and increases with increasing the exposure time.

Also, corrosion rate was calculated from weight loss and presented as a function of inhibitor concentration of the used cationic surfactant in **Fig. 3**. It is clear that, the corrosion rate of the carbon steel was decreased dramatically by increasing the inhibitor concentration and consequently the inhibition efficiencies of the inhibitor increased due to the adsorption of inhibitor on the carbon steel surface.

The value of corrosion inhibition efficiency η_w (%) was determined from weight loss using the following equation [31, 32]:

$$\eta_w \% = (1 - W_{(inh)}/W_{(free)}) \times 100 \quad (1)$$

Where $W_{(free)}$ and $W_{(inh)}$ are the weight loss in the absence and presence of inhibitor, respectively. **Table 1** reports the values of corrosion rate and percentage inhibition efficiency for X-70 type carbon steel immersed in 8 % sulfamic acid solution in the absence and presence of various concentrations of the inhibitor (DDBAB). Inspection of these data in **Table 1**, reveal that increasing the surfactant concentration decrease in the weight loss and the corrosion rate of carbon steel to be the lowest at 150 ppm concentration. This effect is attributed to the formation of a protective layer from the inhibitor molecules on the carbon steel surface.

It is generally agreed that the primary action in the inhibition process by surfactants is the adsorption of the surfactant molecules via their functional group onto the metal surface [33]. Therefore, it was of a particular interest to investigate the phenomenon of adsorption of such compounds and determine the degree of surface coverage (θ) by the adsorbed surfactant molecules.

The degree of surface coverage is calculated from weight loss (θ_{wtloss}) using the following relation as follow [34]:

$$\theta_{wtloss} = 1 - W_{(inh)}/W_{(free)} \quad (2)$$

The values of the degree of surface coverage (θ), the percentage inhibition efficiency (η_w %) and the corrosion rate were calculated for the inhibitor (DDBAB) and summarized in **Table 1**. Also, from the previous data one can conclude that, by increasing the inhibitor concentration, the surface coverage (θ) of metal surface by inhibitor molecules was increased and reached ($\theta = 0.92$ at 150 ppm for DDBAB). This increase in the degree of surface coverage leads to decrease the contact between the metal surface and the aggressive medium and consequently decreases the dissolution of the metal and increasing the inhibition efficiency. The values of the degree of surface coverage (θ) obtained from weight loss measurements for the tested

inhibitor (DDBAB) have been applied to different adsorption isotherms in order to investigate the type of adsorption. For this purpose, C_i/θ is plotted against C_i for the surfactant (DDBAB) as indicated in **Fig. 4**. The experimental results give a straight line with a slope nearly equal the unity, suggesting that the inhibitor molecules adsorbed on the carbon steel immersed in / 8% sulfamic acid obeys the Langmuir adsorption isotherm, which represented by the following equation [35]:

$$C_i/\theta = 1/K_{ads} + C_i \quad (3)$$

Where C_i is the inhibitor concentration and k_{ads} represents the adsorption equilibrium constant of the inhibitor on carbon steel surface. The slope of the isotherm deviates from unity. This deviation is generally attributed to the interaction between the adsorbed inhibitor molecules on carbon steel surface via mutual repulsion or attraction [36-38]. K_{ads} values were calculated from intercepts of the straight lines on the C_i/θ axis [39]. The free energy of adsorption (ΔG°_{ads}) of the inhibitor on the surface of carbon steel was calculated as follows [40, 41]:

$$\Delta G^\circ_{ads} = -RT \ln(55.5 K_{ads}) \quad (4)$$

Where R is the universal gas constant ($8.314 \text{ J mol}^{-1} \text{ K}^{-1}$), T is the absolute temperature (K), and the value 55.5 is the molar concentration of water in solution.

The values of K_{ads} and ΔG°_{ads} of DDBAB inhibitor were listed in **Table 2**. It is clear that, the high value of K_{ads} indicated the strong adsorption ability of the inhibitor on the surface of carbon steel in 8% sulfamic acid. The negative sign of ΔG°_{ads} means that the adsorption of inhibitor on carbon steel surface is spontaneous process, and furthermore the negative values of ΔG°_{ads} also show the strong interaction of the inhibitor molecule onto the carbon steel surface [42,43]. Generally, if the value of ΔG°_{ads} is around -20 kJ mol^{-1} or lower. This is consistent with the electrostatic interaction between inhibitor and the charged metal surface (i.e. physisorption), while that more negative than -40 kJ mol^{-1} involve charge sharing or transfer from the inhibitor molecules to the metal surface to form a coordinate type of bond (i.e. chemisorption) [44]. For the investigated inhibitor (DDBAB), one can see that the calculated value of ΔG°_{ads} equals $-34.19 \text{ kJ mol}^{-1}$, indicated that the adsorption of the dodecyl dimethyl benzyl ammonium bromide (DDBAB) on the carbon steel in 8% sulfamic acid can be regarded as a mixed physical and chemical adsorption (i.e. physicochemical type) [45-47].

3.2. Tafel Polarization measurements:

Fig.5 is showing typical polarization curves for the inhibition characteristics of inhibitor (DDBAB). These curves show anodic and cathodic polarization plots recorded on carbon steel electrode in 8% sulfamic acid at various concentrations in the presence and absence of inhibitor (DDBAB). As would be expected both anodic and cathodic reactions of carbon steel electrode corrosion were inhibited with the increase of inhibitor (DDBAB) concentration. This result suggests that the addition of inhibitor (DDBAB) reduces anodic dissolution and also retards the hydrogen evolution reaction. **Table 3** shows the electrochemical corrosion kinetic parameters, i.e., corrosion potential (E_{corr}), cathodic and anodic Tafel slopes (β_c and β_a), polarization resistance (R_p) and corrosion current density i_{corr} obtained by extrapolation of the Tafel lines. The calculated inhibition efficiency, IE_p (%) is also reported from the following equation [48]:

$$\eta_p(\%) = \left(1 - \frac{i_{\text{corr}}}{i_{\text{corr}}^o}\right) \times 100 \quad (5)$$

Where i_{corr}^o and i_{corr} correspond to uninhibited and inhibited the corrosion current densities, respectively. The best inhibition efficiency was about 91.1% at concentration 150 ppm. It can be seen that by increasing the concentration of inhibitor, the corrosion rate decreased and inhibition efficiency η_p (%) increased. This behavior confirms a greater increase in the energy barrier of the carbon steel dissolution process. It is clear that the used cationic surfactant (DDBAB) affect both the anodic and cathodic reaction so that, it acts as a mixed type inhibitor but the cathodic effect is more pronounced as a slight shift of E_{corr} in the cathodic direction. Moreover, this inhibitor cause no change in the cathodic and anodic Tafel slopes, indicating that the inhibitor is first adsorbed onto carbon steel surface and therefore impedes by merely blocking the reaction sites of iron surface without affecting the anodic and cathodic reaction mechanism [49,50].

3.3. Impedance measurements

The effect of inhibitor (DDBAB) concentrations on the impedance behavior of carbon steel in 8% sulfamic acid solutions is presented in **Fig.6**. These curves show a typical set of Nyquist plots for carbon steel in 8% sulfamic acid solution without and with various concentrations of dodecyl dimethyl benzyl ammonium bromide. It is clear

from these plots that the impedance response of carbon steel has significantly changed after the addition of inhibitor in the corrosive media. This indicates that the impedance of an inhibited substrate increases with increasing concentration of inhibitor in 8% sulfamic acid. It is worth noting that the change in concentration of DDBAB inhibitor did not alter dramatically the profile of the impedance behavior, suggesting similar mechanism for the corrosion inhibition of carbon steel by inhibitor (DDBAB), **Fig.6**. The charge transfer resistance values (R_{ct}) were calculated from the difference between impedance values at lower and higher frequencies as suggested by Tsuru et al. [51]. The impedance parameters derived from **Fig. 6** are given in **Table 4**. The double layer capacitance C_{dl} and inhibition efficiency IE (%) were calculated from the following equations [52, 53]:

$$\eta_I(\%) = \left(1 - \frac{R_{ct}^{\circ}}{R_{ct}}\right) \times 100 \quad (6)$$

$$f(-Z''_{img}) = \frac{1}{2\pi C_{dl}R_{ct}} \quad (7)$$

where R_{ct}° and R_{ct} are the charge transfer resistances in 8% sulfamic acid solution without and with different concentrations of inhibitor, respectively, $f(-Z''_{img})$ is the frequency at maximum imaginary component of the impedance. From **Table 4**, it was clear that charge transfer resistance R_{ct} values were increased and the capacitance C_{dl} values decreased with increasing the concentration of inhibitor. This decrease in the capacitance C_{dl} , which can result from a decrease in local dielectric constant and/or an increase in the thickness of the electrical double layer, suggests that the inhibitor molecules act by adsorption at the carbon steel /sulfamic acid solution interface [54]. The addition of inhibitor (DDBAB) provides lower C_{dl} values, probably as a consequence of replacement of water molecules by the adsorption of inhibitor (DDBAB) at the electrode surface. Also the inhibitor molecules may reduce the capacitance by increasing the double layer thickness according to the Helmholtz model [55]:

$$C_{dl} = \frac{\epsilon\epsilon_0 A}{\delta} \quad (8)$$

Where ϵ is the dielectric constant of the medium, ϵ_0 is the vacuum permittivity, A is the surface area of electrode and δ is the thickness of the protective layer. The value

of C_{dl} is always smaller in the presence of the inhibitor than in its absence, as a result of the effective adsorption of the inhibitor (DDBAB).

It is clear that, η_I was increased with increasing the inhibitor concentration. This fact suggests that the inhibitor molecules may first be adsorbed on the carbon steel surface and cover some sites of the electrode surface. Then probably, they form monomolecular layers on the carbon steel surface. These layers protect carbon steel surface from attack of hydrogen ions and prevent iron dissolution. EIS spectra were analyzed by using the equivalent circuit as illustrated in **Fig. 7**. This figure revealed a single charge transfer reaction. The diameter of the capacitive loop obtained in 8% sulfamic acid solution was increased in the presence of inhibitor indicating an inhibition of the corrosion process.

Fig.8. represents the Bode–phase plot for the dodecyl dimethyl benzyl ammonium bromide for carbon steel in 8 % sulfamic acid solution at 25°C. The frequency range of the Bode–phase plot was used to describe the different phenomena occurring at interfaces, and phase angle at high frequencies was used to provide a general idea for inhibition performance. It is well known that, an ideal capacitive behavior would be the result if phase angle value attained -90° [56]. **Fig. 8** shows an increase of phase angle shift with the increase of inhibitor concentration and thus a gradual approach of phase angle towards the ideal capacitive behavior. The higher values of phase angle for inhibited solution than uninhibited solution reflect the inhibitive action of the dodecyl dimethyl benzyl ammonium bromide.

Variation of the inhibition efficiency with (DDBAB) inhibitor concentration as calculated from three different techniques is presented in **Fig. 9**.

3.4. Surface Morphology Analysis

3.4.1. SEM studies of the carbon steel surface

To confirm the formation of a protective surface film of inhibitor on the carbon steel surface, SEM technique was used to characterize the carbon steel surface. The scanning electron microscope photographs were recorded (**Fig. 10a–c**) to establish the interaction of organic molecules with the carbon steel surface. A photograph of the polished carbon steel surface before immersion in 8% sulfamic acid solution is shown in **Fig. 10 (a)**. The photograph shows that the X 70 surface of carbon steel was smooth and without pits [57, 58]. A photograph of the carbon steel surface after

immersion in 8% sulfamic acid solution is shown in **Fig. 10 (b)**. The photograph reveals that, the X70 surface of carbon steel appeared like full of pits and cavities in the absence of inhibitor. **Fig 10 (c)** shows a photograph of the surface carbon steel in 8% sulfamic acid solution with 150 ppm of inhibitor (DDBAB), showing a protective layer and the surface of carbon steel immersed in inhibitor (DDBAB) was smoother when compared with that in blank **Fig. 10 (b)**. This is because of the formation of an adsorbed film of (DDBAB) inhibitor reducing corrosion of X70 carbon steel in 8% sulfamic acid solution. It can be concluded from **Fig. 10 (a–c)** that the corrosion rate was strongly suppressed in the presence of inhibitor molecules for API X70–type carbon steel surface in 8% sulfamic acid solution.

3.4.2. EDX examinations of the carbon steel surface

EDX survey spectra were used to determine which elements were present on the carbon steel surface before and after exposure to the inhibitor solution. Energy dispersive analysis of X-ray (EDX) was carried out in order to analyze surface composition of the formed protective film. The EDX spectrum of polished carbon steel sample in **Fig. 10 (a)** shows good surface properties, while the EDX spectrum in case of carbon steel sample immersed in 8% sulfamic acid in the absence of inhibitor molecules for 28 hrs was failed because it was severely weakened by external corrosion as shown in **Fig. 10 (b)**. The oxygen signal apparent in **Fig. 10 (b)** is due to the carbon steel surface exposed to the sulfamic acid in the absence of inhibitor (DDBAB). By adding 150 ppm of DDBAB inhibitor, The EDX spectrum of **Fig. 10 (c)** shows that the Fe peak is considerably suppressed relative to the sample prepared in 8 % sulfamic acid solution. The suppression of the Fe peak occurs because of the overlying inhibitor film. These results are confirmed those previously obtained from chemical and electrochemical measurements, which suggest that a surface film inhibited the metal dissolution, and hence retarded the hydrogen evolution reaction. This surface film also increases the charge transfer resistance of the metal dissolution of carbon steel **Fig. 10 (c)**, slowing down the corrosion rate. The protective film formed by inhibitor molecules was strongly, adherent to the surface, which leads to a high degree of inhibition efficiency [59]. Therefore, EDX and SEM examinations of the electrode surface support the results obtained from chemical and electrochemical methods that DDBAB can be regarded as an effective inhibitor for carbon steel in 8% sulfamic acid solutions.

3.5. Quantum Chemical Calculations

The electronic parameters give the information concerning the interaction between inhibitors and carbon steel surface. Quantum chemical calculations are the most used method to understand electronic distribution of inhibitor molecules [60–62]. Frontier orbital theory is useful in predicting adsorption centers of the inhibitor molecules responsible for the interaction with the carbon steel. The optimized molecular structure, electron density and HOMO–LUMO of the DDBAB inhibitor are shown in **Figs. 11(a), 11(b), 11(c) and 11(d)**.

Quantum chemical parameters obtained from the calculations which are responsible for the corrosion inhibition efficiency of inhibitor and are thought important to directly influence on electronic interaction between Fe atoms in surface carbon steel and inhibitor, such as the energy of the highest occupied molecular orbital (E_{HOMO}), energy of the lowest unoccupied molecular orbital (E_{LUMO}), the energy gap ($\Delta E = E_{LUMO} - E_{HOMO}$). ΔE represents the function of reactivity, hardness ($\eta = \Delta E/2$), softness (σ), chemical potential (π), electronegativity (χ), dipole moment (μ) and the number of transferred electrons from inhibitor atoms to carbon steel surface (ΔN) all are collected in **Table 5**.

According to Koopman's theorem [63], the energy of HOMO (E_{HOMO}) of the inhibitor molecules is directly related to the ionization potential (IP) and characterizes the susceptibility of the molecule towards the attack by electrophiles.

$$IP = -E_{HOMO} \quad (9)$$

The energy of LUMO (E_{LUMO}), which stands for the ability of electron receiving tendency, is directly related to the electron affinity (EA) and characterizes the susceptibility of the molecule towards the attack by nucleophiles [64, 65].

$$EA = -E_{LUMO} \quad (10)$$

Other quantum chemical parameters that give valuable information about the reactive behavior of the inhibitor such as the electronegativity (χ), chemical potential (π), hardness (η) and softness (σ) were calculated by the following relations [66]:

$$\chi = -\pi = \frac{-(E_{HOMO} + E_{LUMO})}{2} = \frac{IP + EA}{2} \quad (11)$$

$$\eta = \frac{\Delta E}{2} = \frac{(E_{LUMO} - E_{HOMO})}{2} = \frac{IP - EA}{2} \quad (12)$$

The inverse of the global hardness is designated as the softness, σ as follows:

$$\sigma = \frac{1}{\eta} = \frac{2}{\Delta E} = \frac{2}{(E_{LUMO} - E_{HOMO})} = \frac{2}{IP - EA} \quad (13)$$

The number of transferred electrons (ΔN) was also calculated depending on the quantum chemical method according to the following equation [62, 63]:

$$\Delta N = \frac{X_{Fe} - X_{inh}}{2(\eta_{Fe} + \eta_{inh})} \quad (14)$$

Where X_{Fe} and X_{inh} denote the absolute electronegativity of iron and the inhibitor molecule, respectively; η_{Fe} and η_{inh} denote the absolute hardness of iron and the inhibitor molecule, respectively. Quantum chemistry calculations in **Table 5** reveal that the lower is the value of the E_{LUMO} of the inhibitor, the easier the acceptance of electrons from atoms in carbon steel surface, which decreases the energy gap and improves the corrosion efficiency of inhibitor. The higher is the value of the E_{HOMO} of the inhibitor, implying the ability of this molecule to offer free electrons to unoccupied d-orbital of the Fe atoms, which decreases the energy gap (ΔE) and increases the corrosion efficiency of inhibitor for iron in 8% sulfamic acid solutions. In other words, the inhibition efficiency increases if the inhibitor can donate electrons to the metal surface. In addition, the dipole moment (μ), the first derivative of the energy with respect to an applied electric field, is an index that can also be used for the prediction of the direction of a corrosion inhibition process [68]. High values of the dipole moment will favor the accumulation of inhibitor molecules on the surface carbon steel.

The energy gap, ΔE approach, which is an important stability index, was applied to develop theoretical models for explaining the structure and conformation barriers in many molecular systems. The energy band gap decreased and the corrosion efficiency of inhibitor improved, because the energy needed to remove an electron from the last occupied orbital will decreased and hence the ionization potential will be low [69]. The values of ΔE in **Table 5**, suggesting the strongest ability of the DDBAB inhibitor to form coordinate bonds with d-orbitals of carbon steel surface through donating and accepting electrons, is in good agreement with the experimental results. Absolute hardness, η , and softness, σ , are important properties which measure both the stability and reactivity of a molecule. A hard molecule has a large energy gap and a soft

molecule has a low energy gap. Soft molecules are more reactive than hard molecules because they could easily offer electrons to an acceptor. The energy gap indicates that the smaller energy gap results in a high corrosion inhibition implying soft–soft interaction of inhibitor on the carbon steel surface. For the simplest transfer of electrons, adsorption should occur at the part of the molecule where the softness, σ , which is a local property, has the highest value [70].

In a corrosion system, the iron surface acts as a Lewis acid (electron acceptor) while the inhibitor acts as a Lewis base (electron donor), respectively. Bulk iron surface is soft acids and thus inhibitor behaves as soft base (proton acceptor) is most effective for corrosion of carbon steel in 8% sulfamic acid. Accordingly, it was concluded that inhibitor DDBAB with the highest σ value (1.6584 eV^{-1}) has the highest inhibition efficiency, **Table 5**, which agrees well with the experimental data.

The electronegativity value will decrease with the enhancement of inhibitive efficiencies, as shown in **Table 5**, because good inhibitor donates electron to the atoms in carbon steel surface. Using a theoretical X_{Fe} value of 7 eV/mol and η_{Fe} value 0 eV/mol [71], the fraction of electrons transferred from inhibitor to atoms in carbon steel surface (ΔN) was calculated and listed in **Table 5**. The positive number of electrons transferred (ΔN) exhibits that the molecules operate as an electron donor, while a negative number of electrons transferred (ΔN) indicates that the molecules have activity as electron acceptors [72]. The values of (ΔN) in **Table 5** indicated that the DDBAB inhibitor act as electron donors and a higher ΔN implies a very large tendency to interact with atoms of metal surface. The values of ΔN are less than 3.6, which indicate based on Lukovits's study that the inhibition efficiency increased with increasing electron-donating ability of inhibitor at the surface carbon steel. In this study, the DDBAB inhibitor was the electron donor, and the iron surface was the electron acceptor. The DDBAB inhibitor was bound to the surface of carbon steel by adsorbing on it and thus formed inhibition adsorption layer which decreases the corrosion.

The inhibitor may adsorb on the surface carbon steel atoms in the form of cation and share electrons between the nitrogen atoms in inhibitor molecule and the atoms in carbon steel surface. The other possibility is that the inhibitor molecules are adsorbed

through electrostatic interaction between negatively charged carbon steel surfaces and positively charged of the inhibitor molecules [73].

It was shown from **Fig. 11(a)** that the DDBAB inhibitor is nearly a planar structure, which can offer the largest contact area between the atoms in surface carbon steel and the inhibitor molecules. The inhibiting effect of this inhibitor was attributed to its parallel adsorption at the surface carbon steel by active centers of adsorption. Due to the planar geometry of the inhibitor, the molecular adsorption probably occurs in such a way that the surface metal atoms and the molecular plane are parallel to each other by donation and back donation between the molecule and the carbon steel surface.

Furthermore, the HOMO level of the DDBAB inhibitor is mostly localized on the phenyl moiety and the nitrogen atom, which indicates that phenyl moiety and the nitrogen atom are the preferred sites for the electrophilic attack on the carbon steel surface and are probably the primary sites of the bonding at the carbon steel surface, **Fig. 11(c)**. This means that the phenyl moiety and the nitrogen atom with high coefficients of HOMO density are oriented towards the carbon steel surface and the adsorption probably occurred through the π -electrons of the phenyl moiety and the lone pair electrons of the nitrogen atom. Also, the calculations showed that the charge density of the LUMO level is completely delocalized on the phenyl moiety and the nitrogen atom for DDBAB inhibitor which means that this phenyl moiety and the nitrogen atom could be reacted as electrophile, Lewis base, (electron donor), **Fig. 11(d)**. It is concluded that the region of active centers transforming electrons from N atoms to iron surface of carbon steel. The electron configuration of iron is [Ar] $4s^23d^6$; the 3d orbitals are not fully filled with electrons. N atoms have lonely electron pairs that are important for bonding unfilled 3d orbitals of iron atom and determining the adsorption of the molecules on the metal surface. There is a general consensus by several authors that the more positively charged heteroatom is, the more it can be adsorbed on the iron surface of carbon steel through donor–acceptor type reaction [74, 75].

The molecular electrostatic potential (MEP) is related to the electronic density and is a very helpful in the negative region can be regarded as electrophilic centers, whereas region with positive electrostatic potential is potential nucleophilic sites. Moreover, the electrostatic potential makes the polarization of the electron density visible. The

calculations showed that the phenyl moiety and the nitrogen atom have negative electrostatic potential which means that these sites are the active centers for the binding to the carbon steel surface, **Fig. 12**. The structure of the DDBAB inhibitor has phenyl ring which acts as an electron withdrawing group, increases the delocalization of the electron cloud on the molecule which enhances its adsorption and improved the corrosion inhibition efficiency. The structure of the inhibitor molecules can affect the adsorption by influencing the electron density at the functional group; the regions of high electron density are generally the sites which electrophilic attack. The electron density focused on the N atom and the phenyl moiety. This means that these regions have the strongest ability of bond to the metal surface.

3.6. Surface active characteristics

The surface tension (γ) of the various concentrations of the DDBAB cationic surfactant (inhibitor) was measured. The relationship between surface tension (γ) and log concentration ($\log C$) of the cationic surfactants is shown in **Fig. 13**. From the obtained curve, it was found that, a significant decrease in surface tension was observed with the increase of the surfactant concentration until CMC is reached above which the surface tension is not affect by a further increase in the surfactant concentration. The surface active properties of the DDBAB cationic surfactants were calculated and summarized in **Table 6**. The critical micelle concentration (CMC) value of the DDBAB cationic surfactant ($1.78 \times 10^{-3} \text{ mol dm}^{-3}$) was estimated from the intersection point in the γ - $\log C$ plot. It is clear that CMC plays an effective boundary condition below which, the adsorption of surfactant molecules is typically below the mono-layer level and above which multi-layer of physically adsorbed surfactant molecule can exist[76], and lowering CMC leads to better solubility which normally relies on the surfactant concentration in the solution bulk phase [77]. The data showed that the DDBAB cationic surfactant is considered as a strong surface active agent at air – water interface.

The effectiveness of the DDBAB cationic surfactant (39.3 mN m^{-1}) is good for lowering the surface tension of pure water (72.3 mN m^{-1}) to the detected value (33 mN m^{-1}).The explanation of this result was attributed to the structure of the DDBAB cationic surfactant and the strong binding ability of its counter ion (Bromide ion).The surface excess concentration value was $1.66 \times 10^{-10} \text{ mol cm}^{-2}$. This date means that, by increasing the hydrophobic chain length, as in the case of dodecyl dimethyl benzyl

ammonium bromide, the hydrophobicity increases. Therefore, the DDBAB cationic surfactant molecules are directed to the interface and the surface energy of the solution decreases. This attitude supposed leads to an increase in the maximum surface excess [78].

The surface activity of the DDBAB cationic surfactant result revealed that the surface pressure ($\pi_{\text{CMC}} = 39.3 \text{ mN m}^{-1}$) of the cationic surfactant increases with decreasing the minimum surface area ($A_{\text{min}} = 100 \text{ \AA}^2$) of the adsorbed surfactant molecules [79]. The low value of A_{min} suggested that the surfactant molecules at air/water interface are close-packed; therefore, the orientation of the surfactant molecule at the interface was almost perpendicular to the interface leading to the low surface tension in CMC.

The surface active characteristic results showed that the negative value of $\Delta G_{\text{ads}}^{\circ}$ and $\Delta G_{\text{mic}}^{\circ}$ of the DDBAB cationic surfactant. This result indicated that the spontaneously of these two processes in the aqueous phase, i.e., the adsorption and micellization processes occurred in the solution in an exothermic process without the need of energy. On the other side, the value of $\Delta G_{\text{ads}}^{\circ}$ is more negative than the value of $\Delta G_{\text{mic}}^{\circ}$, which indicated that the DDBAB cationic surfactant prefer to be adsorbed at air/water interface than to make micelles in the bulk solution. The adsorption tendency is reflected from the sharp decrease in the surface tension values by small increase in their concentration [80].

3.7. Corrosion inhibition mechanism

The cationic surfactant molecules are adsorbed on carbon steel surface through Van der Waals attraction force between the head groups and the surface of carbon steel, in addition to the formation of $p\pi$ - $d\pi$ bond between the filled p-orbital of the surfactant molecules and the vacant d-orbital of steel surface, **Fig. 14 (a)**. So that one can conclude that the increase in inhibition efficiency achieved at higher inhibitor concentrations indicates that more inhibitor molecules were adsorbed on the metal surface, thus, providing wider surface coverage which demonstrates that this compound acts as an adsorption inhibitor, **Fig. 14 (b)**. Meanwhile at the over dose concentration (at maximum inhibition efficiency obtained), the inter space area between the adsorbed inhibitor molecules on the surface may be lesser than the area of the inhibitor molecules. So that the inhibitor molecules turn out to form the double layer adsorption as shown in **Fig. 14 (c)** [81].

4. Conclusions

The main conclusions of the present study can be stated in the following points:

- The cationic surfactant namely, dodecyl dimethyl benzyl ammonium bromide (DDBAB) acts as an effective inhibitor for the corrosion of carbon steel in 8% sulfamic acid solution.
- The corrosion inhibition efficiency is due to adsorption of the inhibitor molecules on the carbon steel surface according to the Langmuir's adsorption isotherm and blocking its active sites.
- Weight loss data showed that addition of DDBAB decreases the dissolution and corrosion rate of carbon steel even after 28 h of the coupons immersion; this effect increases upon increasing the DDBAB concentration.
- Potentiodynamic polarization curves indicated that the selected compound suppresses both anodic and cathodic process and thus acts as a mixed-type inhibitor.
- The results of EIS indicate that the value of C_{dl} tends to decrease and both R_{ct} and $\eta\%$ tends to increase by increasing the inhibitor concentration. This result can be attributed to increase of the thickness of the electrical double layer.
- Results obtained from DC polarization, AC impedance and weight loss techniques are in reasonably good agreement and show increased inhibition efficiency with increasing inhibitor concentration.
- The surface active properties of the cationic surfactants were calculated from surface tension measurements.
- Quantum chemical calculations shows that the inhibition effect of DDBAB is mainly attributed to mixed adsorption mechanism assisted by H-bond formation with the carbon steel surface.
- Quantum chemical calculations revealed that the inhibition efficiency of inhibitor increased with the increase in E_{HOMO} and decrease in $E_{HOMO}-E_{LUMO}$.
- The areas containing N atom and phenyl moieties are most possible sites for bonding the metal iron surface by donating electrons to the metal.
- The adsorption of dodecyl dimethyl benzyl ammonium bromide (DDBAB) on carbon steel surface occur directly via donor-acceptor interactions between π -electrons of the phenyl moieties and the vacant d-orbitals of carbon steel or by

electrostatic attraction force between positively charged nitrogen atoms and negatively charged carbon steel surface.

- Surface analysis tools such as SEM and EDX indicated that the DDBAB inhibitor molecules formed a good protective film on the carbon steel surface which isolates the surface from the aggressive environment.
- The smaller band gap favors the adsorption of the DDBAB cationic surfactant on iron surface and enhancement of corrosion inhibition.
- The data obtained from the experimental chemical and electrochemical results are confirmed by theoretical data obtained from quantum chemical calculations.

References

- [1] D. Jayaperumal, S. Muralidharan, P. Subramanian, G. Venkatachari and S. Senthilvel, *Anti-Corros. Meth. Mat.*, 1997, **44** (4), 265 – 268.
- [2] S. Zhang, Z. Tao, W. Li and B. Hou, *Appl. Surf. Sci.*, 2009, **255**, 6757–6763.
- [3] M. Abdallah, *Corros. Sci.*, 2004, **46** (8), 1981–1996.
- [4] M.S. Morad, *J. Appl. Electrochem.*, 2008, **38** (11), 1509–1518.
- [5] M.A. Migahed and I.F. Nassar, *Electrochim. Acta*, 2008, **53** (6), 2877–2882.
- [6] J.R. Kish, N.J. Stead and D.L. Singbeil, *Corrosion*, 2009, **65** (7), 491–500.
- [7] T. Shahrabi, H. Tavakholi and M.G. Hosseini, *Anti-Corros. Meth. Mat.*, 2007, **54**(5), 308–313.
- [8] M. Mahdavian and S. Ashhari, *Electrochim. Acta*, 2010, **55**(5), 1720–1724.
- [9] P. Zhao, Q. Liang and Y. Li, *Appl. Surf. Sci.*, 2005, **252**(5), 1596–1607.
- [10] M. A. Migahed, M. M. Shaban, A. A. Fadda, Tamer Awad Ali and N. A. Negm, *RSC Adv.*, 2015, **5**, 104480–104492.
- [11] K.F. Khaled and M.A. Amin, *Corros. Sci.*, 2009, **51**, 2098–2106
- [12] M. Motamedi, A.R. Tehrani-Bagha and M. Mahdavian, *Corros. Sci.*, 2013, **70**, 46–54
- [13] M. Motamedi, A.R. Tehrani-Bagha and M. Mahdavian, *Electrochim. Acta*, 2011, **58**, 488–496
- [14] A.A. Hermas and M.S. Morad, *Corros. Sci.*, 2008, **50** (9), 2710–2717.
- [15] K.F. Bonhoffer and K. E. Heascer, *Z. Phys. Chem. N.F.*, 1956, **8**, 390.
- [16] N.D. Greene (Ed.), *Experimental Electrode Kinetics*, Rensselaer Polytechnic Institute, New York, 1963.

- [17] X. Liu, S. Houyi Ma, G. Liu and L. Shen, *Appl. Surf. Sci.*, 2006, **235**, 814.
- [18] N.M. Van Os, Non-ionic surfactant “organic chemistry”, Surfactant Science Series, vol72, Marcel Dekker, New York, 1998.
- [19] M.A. Amin, *J. Appl. Electrochem.*, 2006, **36**(2), 215–226.
- [20] J. Vosta, J. Eliasek, and P. Knizek, *Corrosion*, 1976, **32**(5), 183–187.
- [21] Y. Tang, X. Yang, W. Yang, R. Wan, Y. Chen, and X. Yin, *Corros. Sci.*, 2010, **52**(5), 1801–1808.
- [22] Y. Tang, X. Yang, W. Yang, Y. Chen, and R. Wan, *Corros. Sci.*, 2010, **52**(1), 242–249.
- [23] S. M. A. Hosseini, M. Salari, E. Jamalizadeh, and A. H. Jafari, *Corrosion*, 2012, **68**(7), 600–609.
- [24] B. Delley, *J. Chem. Phys.*, 2000, **113**(18), 7756–7764.
- [25] Modeling and Simulation Solutions for Chemicals and Materials Research, Materials Studio (Version 7.0), Accelrys software Inc., San Diego, USA, 2011. <<http://www.accelrys.com>>.
- [26] W.J. Hehre, L. Radom, P.V.R. Schlyer, J.A. Pople, Ab Initio Molecular Orbital Theory, John Wiley, New York, 1986.
- [27] A. Kessi and B. Delley, *Int. J. Quantum Chem.*, 1998, **68**(2), 135–144.
- [28] B. Hammer, L.B. Hansen, and J.K. Nørskov, *Phys. Rev. B*, 1999, **59** (11), 7413–7421.
- [29] A. Matveev, M. Staufer, M. Mayer, and N. Rösch, *Int. J. of Quantum Chem.*, 1999, **75** (4-5), 863–873.
- [30] N. A. Negm, A. F. El Farargy, A. M. Al Sabagh and N, R, Abdelrahman, *J. Surfact. Deterg.*, 2011, **14** (4), 505–514
- [31] Z. Tao, S. Zhang, W. Li and B. Hou, *Corros. Sci.*, 2009, **51**(11), 2588-2595.
- [32] I. Aiad, M.M. El-Sukkary, E.A. Soliman, M.Y. El-Awady, S.M. Shaban, *J. Ind. Eng. Chem.*, 2014, **20** (5), 3524-3535.
- [33] I. L. Rozenfeld, *Corrosion Inhibitors*, McGraw-Hill, New York, 1981.
- [34] I. Ahamad and M.A. Quraishi, *Corros. Sci.*, 2009, **51**(9), 2006-2013.
- [35] S.A. Abd El-Maksoud and A.S. Fouda, *Mater. Chem. Phys.*, 2005, **93** (1), 84-90.
- [36] A. S. Fouda, H. A. Mostafa, M. N. Moussa and Y. M. Darwish, *Bull. Soc. Chem. France*, (1987), **2**, 261.
- [37] A. A. Abdul-Azim, L. A. Shalaby and H. Abbas, *Corros. Sci.*, 1974, **14** (1), 21-24.
- [38] I. B. Obot and N.O. Obi-Egbedi, *Port. Electrochim. Acta*, 2009, **27**(4), 517–524.

- [39] F. Tang, X. Wang, X. Xu and L. Li, *Colloids Surf. A*, 2010, **369** (1-3), 101–105.
- [40] G. Quartarone, M. Battilana, L. Bonaldo and T. Tortato, *Corros. Sci.*, 2008, **50** (12), 3467–3474.
- [41] P. Morales-Gil, G. Negrón-Silva, M. Romero-Romo, C. Ángeles-Chávez, M. Palomar-Pradavé, *Electrochim. Acta*, 2004, **49** (26), 4733–4741.
- [42] M. Abdallah, *Corros. Sci.*, 2002, **44**(4), 717–728.
- [43] Y.S. Ding, M. Zha, J. Zhang and S. S. Wang, *Colloids Surf. A*, 2007, **298** (3), 201–205.
- [44] P. Kuteja, J. Vosta, J. Pancir and N. Hackerman, *J. Electrochem. Soc.*, 1995, **142** (6), 1847–1850.
- [45] M.A. Migahed, R.O. Aly and A.M. Al-Sabagh, *Corros. Sci.*, 2004, **46** (10), 2503–2516.
- [46] P.C. Okafor and Y. Zheng, *Corros. Sci.*, 2009, **51** (4), 850–859.
- [47] M. Behpour, S.M. Ghoreishi, N. Soltani, M. Salavati-Niasari, M. Hamadani, and A. Gandomi, *Corros. Sci.*, 2008, **50** (11), 2172–2181.
- [48] K. Bhrara, H. Kim and G. Singh, *Corros. Sci.*, 2008, **50** (10), 2747–2754.
- [49] M.N.H. Moussa, A.A. El-Far and A.A. El-Shafei, *Mater. Chem. Phys.*, 2007, **105** (1), 105–113.
- [50] K. C. Emregül and M. Hayvalı, *Corros. Sci.*, 2006, **48** (4), 797–812.
- [51] S. Haruyama, T. Tsuru, and B. J. Gijutsu, *Jap. Soc. Corros. Eng.*, 1978, **27** 573–581.
- [52] M. A. Migahed, A. M. Al-Sabagh, E. G. Zaki, H. A. Mostafa and A.S. Fouda, *Int. J. Electrochem. Sci.*, 2014, **9**, 7693–7711.
- [53] G.E. Badr, *Corros. Sci.*, 2009, **51** (11), 2529–2536.
- [54] Y. Tang, X. Yang, W. Yang, Y. Chen and R. Wan, *Corros. Sci.*, 2010, **52** (1), 242–249.
- [55] E.E. Oguzie, Y. Li and F.H. Wang, *Electrochim. Acta*, 2007, **53**(2), 909–914.
- [56] M.A. Hegazy, Ahmed Abdel Nazeer and K. Shalabi, *J. Mol. Liq.*, 2015, **209**, 419–427
- [57] S. Deng and X. Li, *Corros. Sci.*, 2012, **55**, 407–415.
- [58] ASTM E 45-87, Annual Book of ASTM Standard, vol. 11, ASTM, Philadelphia, PA, 1980, p. 125.
- [59] M. A. Amin, S. S. Abd El-Rehim, E.E.F. El-Sherbini and R. S. Bayoumi, *Electrochim. Acta*, 2007, **52** (11), 3588–3600.

- [60] F. Bentiss, M. Lagrenee, B. Elmehdi, B. Mernari, M. Traisnel and H. Vezin, *Corrosion*, 2002, **58**(5), 399–407.
- [61] K. F. Khaled, *Corros. Sci.*, 2010, **52**(10), 3225–3234.
- [62] I. Lukovits, E. Kalman, and F. Zucchi, *Corrosion*, 2001, **57**(1), 3–8.
- [63] V.S. Sastri, and J.R. Perumareddi, *Corrosion*, 1997, **53**(8), 617–622.
- [64] S. Zor, M. Saracoglu, F. Kandemirli, and T. Arslan, *Corrosion*, 2011, **67**(12), 125003-1–125003-11.
- [65] L. A. F. Costa, H. S. Breyer, and J. C. Rubim, *Vibrational Spectroscopy*, 2010, **54**(2), 103–106.
- [66] R.R. Zaky, K.M. Ibrahim, H.M. Abou El-Nadar and S.M. Abo-Zeid, *Spectrochim. Acta Part A*, 2015, **150**, 40–53
- [67] C. Hansch and A. Leo, *Substituentz for Correlation Analysis in Chemistry and Biology*; Wiley: New York, NY, USA, 1979.
- [68] L.R. Ana, Silva, Victor M.F. Morais, Maria D.M.C. Ribeiro da Silva, *J. Mol. Struct.*, 2014, **1078**, 197–206.
- [69] K.F. Khaled, *Appl. Surf. Sci.*, 2008, **255** (5), 1811–1818.
- [70] S. Martinez, *Mater. Chem. Phys.*, 2002, **77** (1), 97–102.
- [71] H. Ju, Z. Kai and Y. Li, *Corros. Sci.*, 2008, **50** (3), 865–871.
- [72] E. El Ashry, A. El Nemr and S. Ragab, *J. Mol. Model.*, 2012, **18** (3), 1173–1188.
- [73] A. Lalitha, S. Ramesh and S. Rajeswari, *Electrochim. Acta*, 2005, **51** (1), 47–55.
- [74] G. Bereket, C. Ogretic and C. Ozsahim, *J. Mol. Struct. (THEOCHEM)*, 2003, **663**, 39–46.
- [75] M.A. Hegazy and F.M. Atlam, *J. Mol. Liq.*, 2016, **218**, 649–662.
- [76] M. A. Migahed, N. A. Negm, M. M. Shaban, T. A. Ali and A. A. Fadda, *J. Surfact. Deterg.*, 2016, **19**(1), 119–128.
- [77] M.J. Rosen, *Surfactants and Interfacial Phenomena*, 2nd ed., Wiley, New York, 1992.
- [78] Th. Dam, J.B.F.N. Engberts, J. Karthäuser, S. Karaborni, N.M. van Os, *Colloids Surf. A*, 1996, **118** (1-2), 41–49
- [79] N. A. Negm and A. S. Mohamed, *J. Surfact. Deterg.*, 2008, **11**(3), 215–221.
- [80] M. Behpour, S.M. Ghoreishi, N. Soltani and M.S. Niasari, *Corros. Sci.*, 2009, **51**(5), 1073–1082.
- [81] A. M. Al-Sabagh, M. A. Migahed, M. Abd El-Raouf, *Chem. Eng. Comm.*, 199 (2012), 737–750.

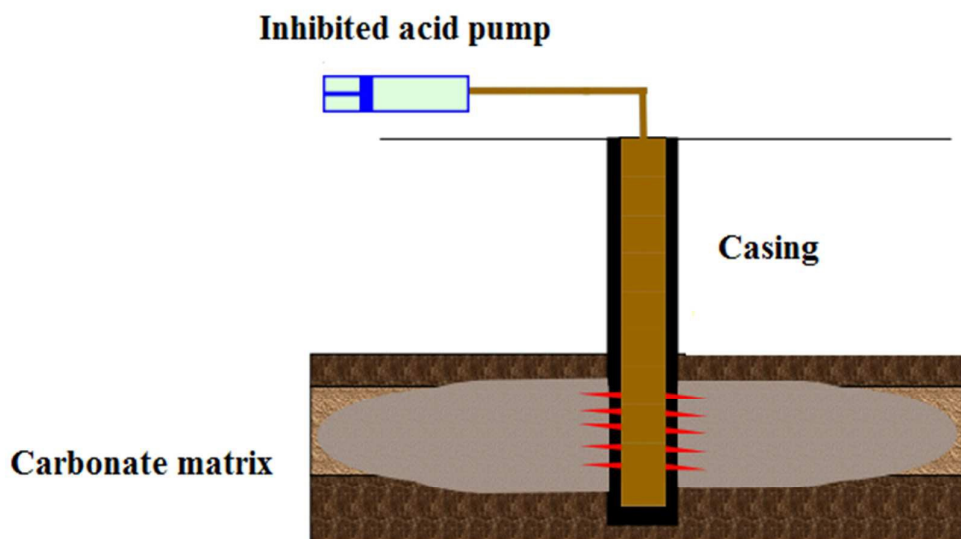


Fig. 1. Cross-section of matrix acidizing process of old oil wells .

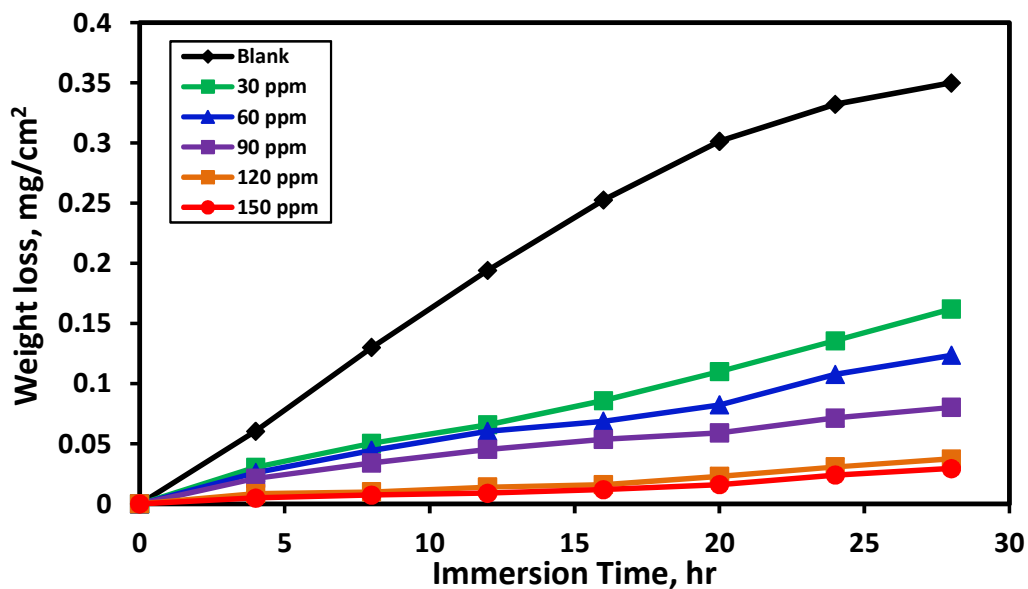


Fig. 2. Effect of exposure time on the weight loss of carbon steel immersed in 8 % sulfamic acid solution in the absence and presence of different concentrations of the inhibitor (DDBAB)

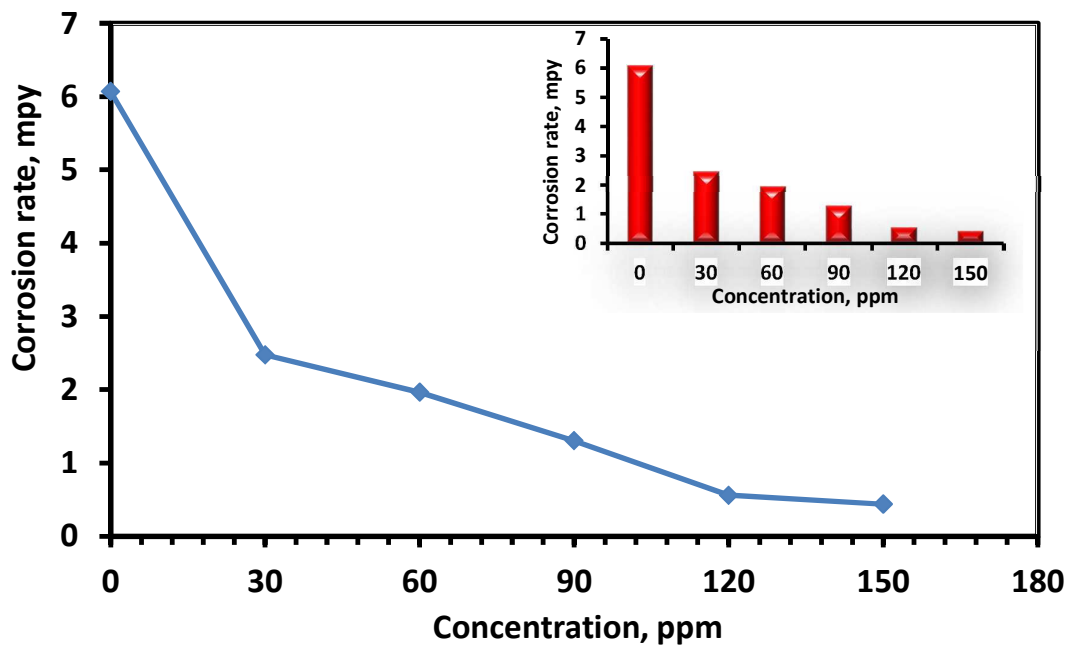


Fig.3. Effect of inhibitor concentration on the corrosion rate of carbon steel in 8% sulfamic acid solution at 25 °C.

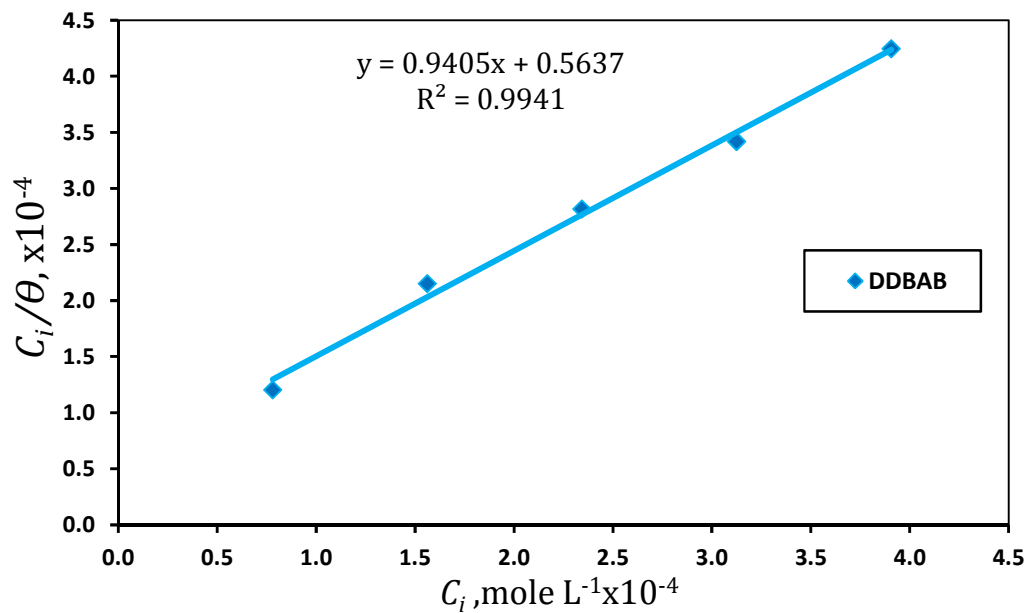


Fig.4. Langmuir adsorption isotherm (C_i/θ vs. C_i) of the inhibitor (DDBAB) on carbon steel surface in 8% sulfamic acid solution

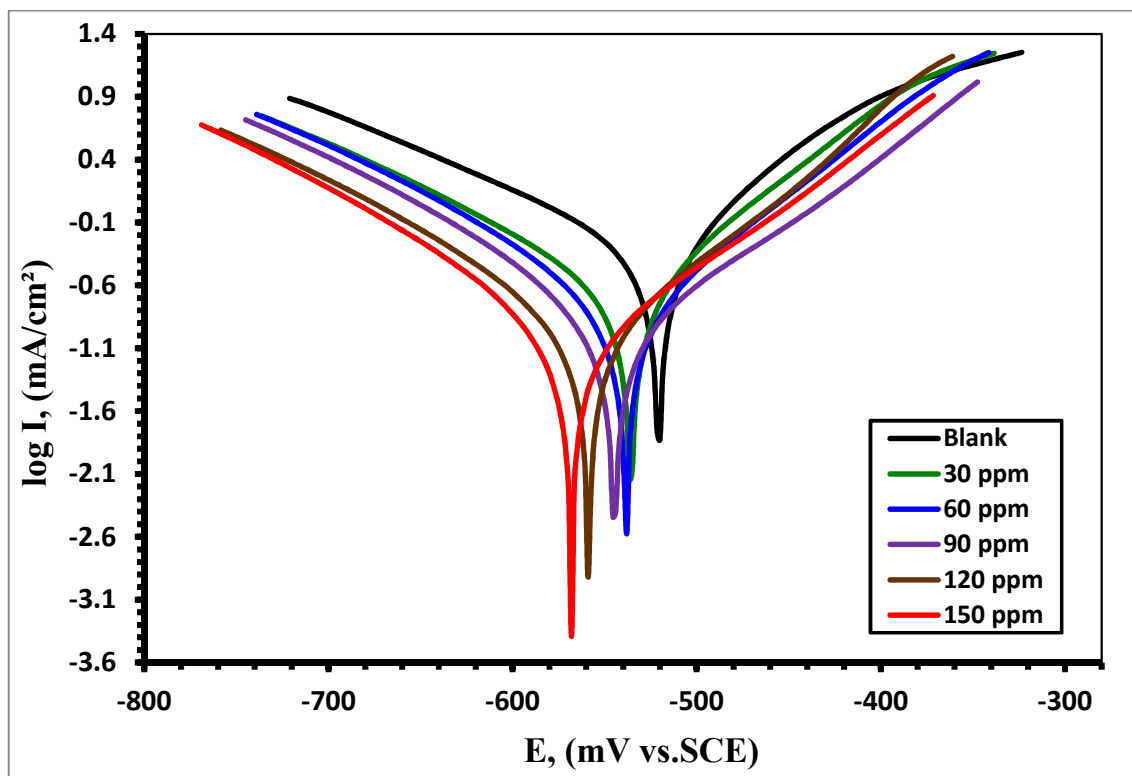


Fig.5. Anodic and cathodic polarization curves of the carbon steel electrode in 8 % sulfamic acid solution without and with various concentrations of inhibitor (DDBAB)

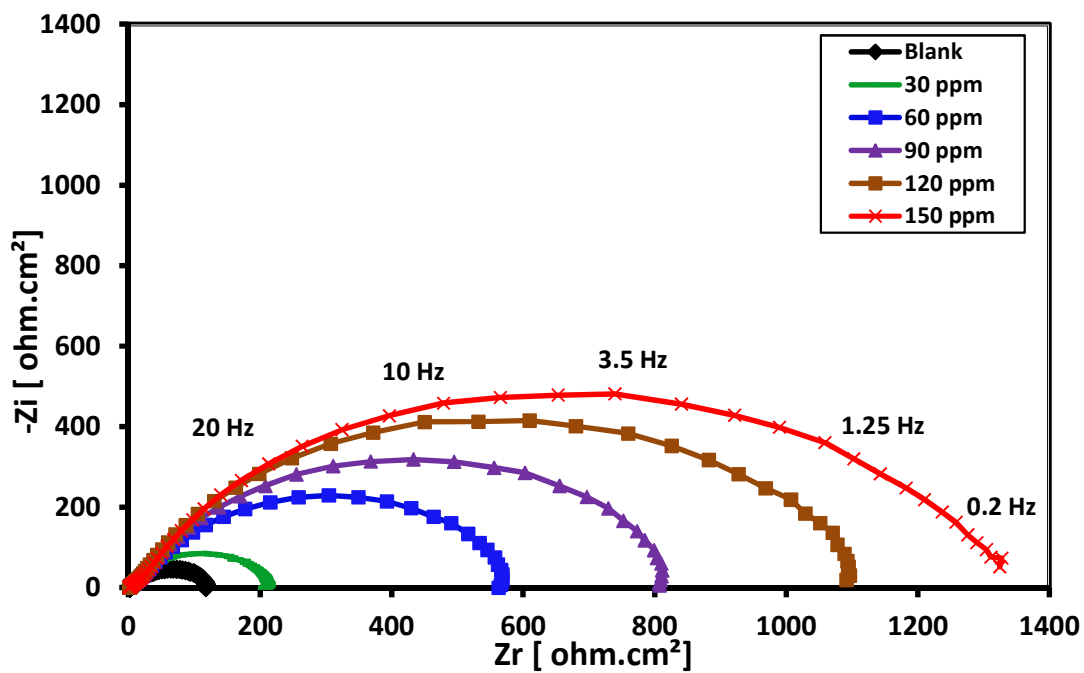


Fig.6. Nyquist plots for the corrosion of carbon steel electrode in 8 % sulfamic acid solution without and with various concentrations of inhibitor (DDBAB)

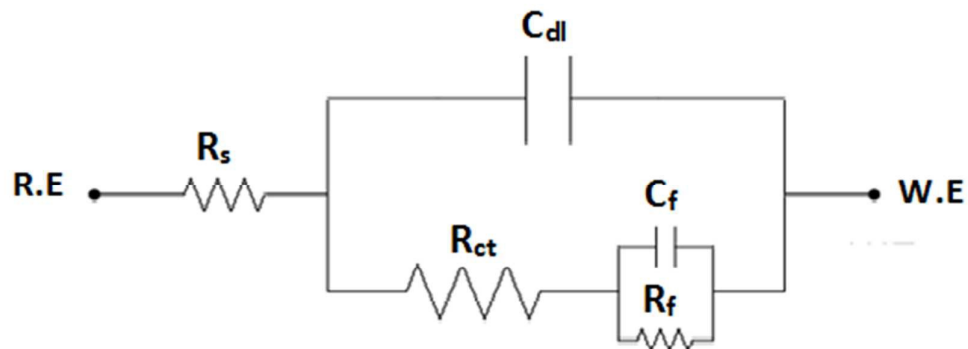


Fig.7. Equivalent circuit used to fit the impedance data for carbon steel in 8 % sulfamic acid solution

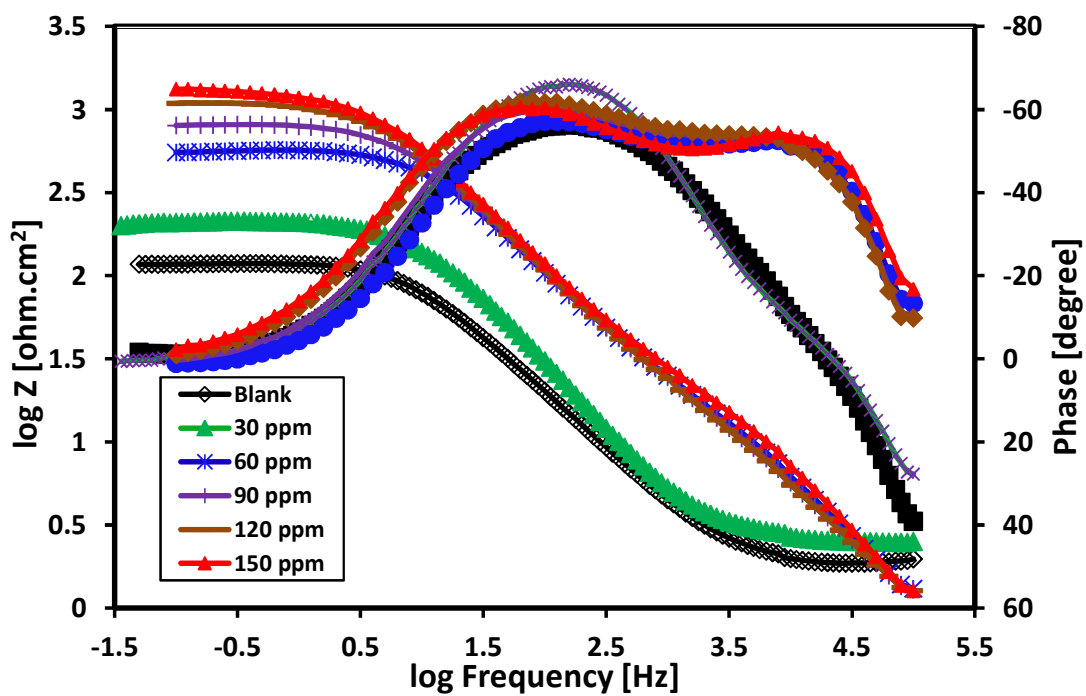


Fig.8. Bode and phase angle plots of carbon steel electrode in 8 % sulfamic acid solution without and with various concentrations of inhibitor (DDBAB)

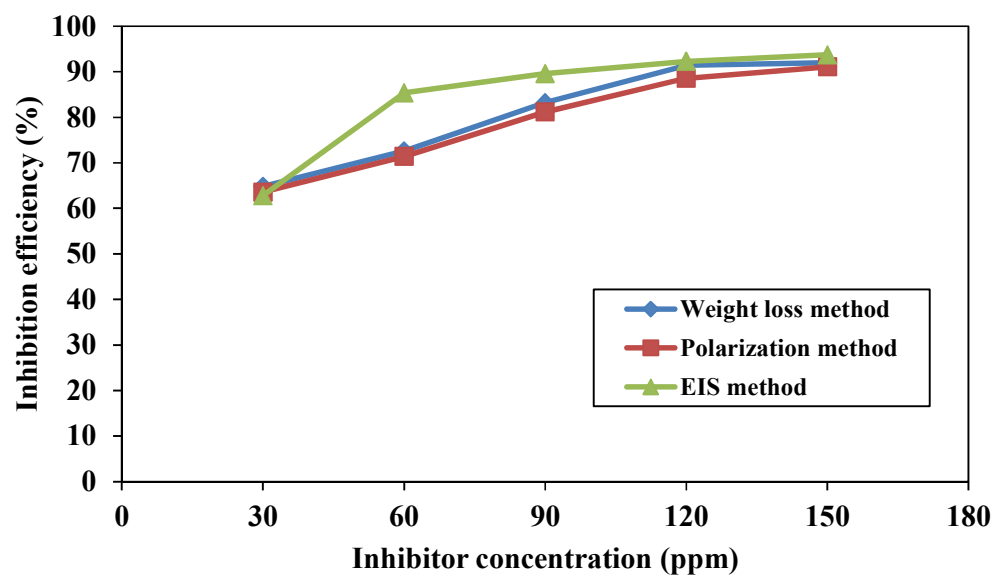


Fig.9. Variation of the inhibition efficiency with inhibitor concentration as calculated from three different techniques.

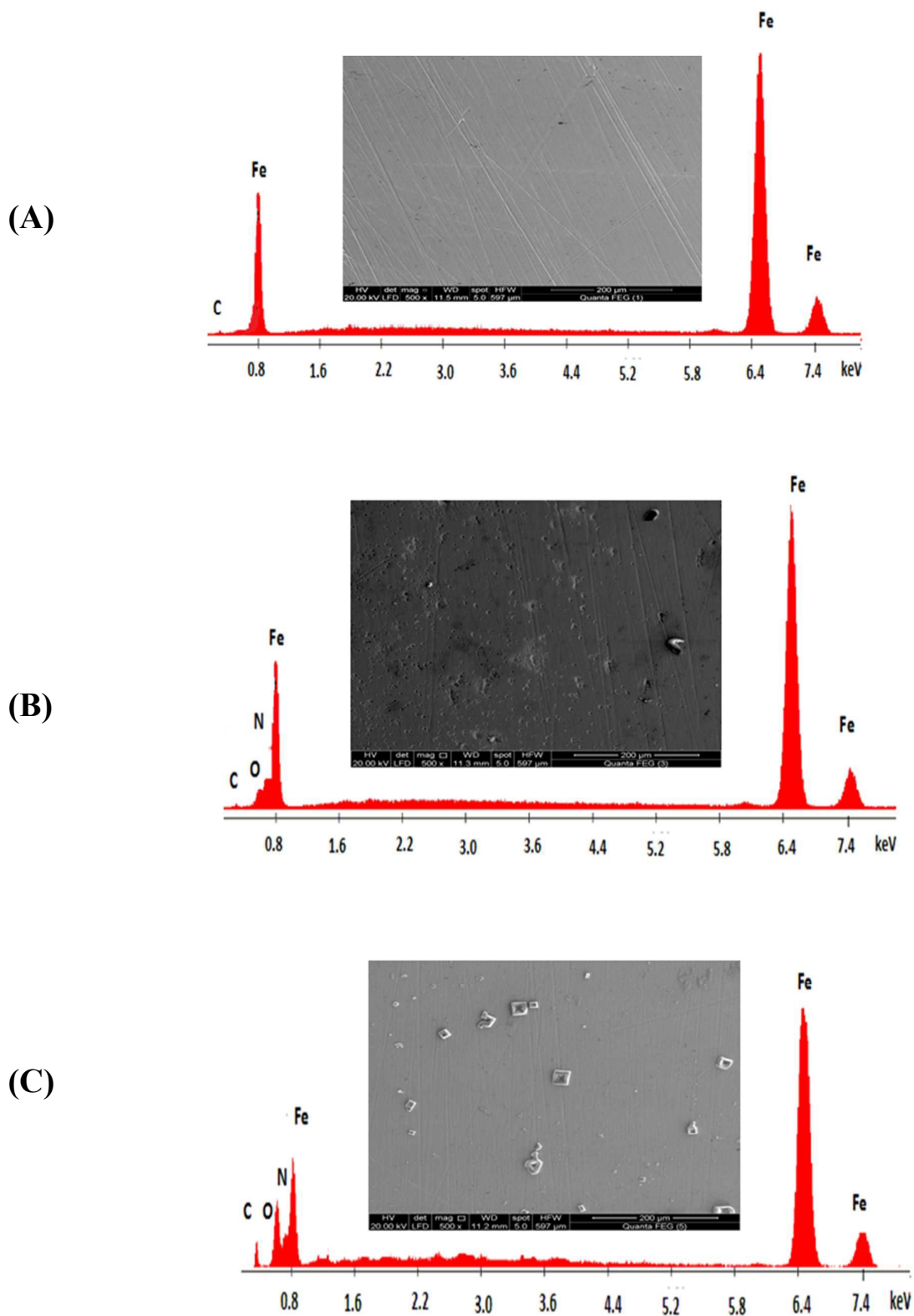


Fig.10. SEM and EDX for carbon steel surface: (A) polished sample, (B) sample immersed in 8% sulfamic acid solution without inhibitor, (C) sample immersed in 8% sulfamic acid solution with 150 ppm of DDBAB inhibitor.

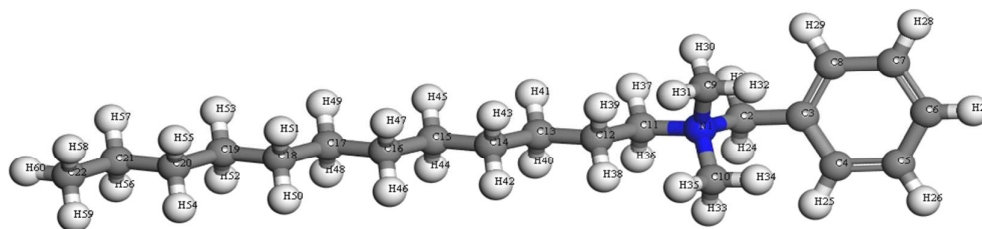


Fig. 11(a): The optimized molecular structure of dodecyl dimethyl benzyl ammonium bromide (DDBAB) inhibitor.

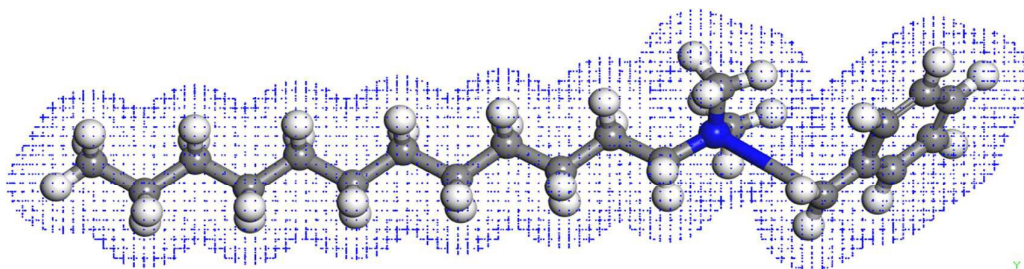


Fig. 11(b): Electron density of dodecyl dimethyl benzyl ammonium bromide (DDBAB) inhibitor

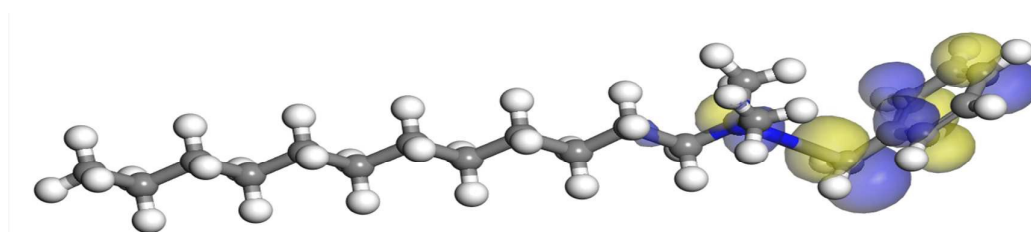


Fig.11(c): HOMO of dodecyl dimethyl benzyl ammonium bromide (DDBAB) inhibitor

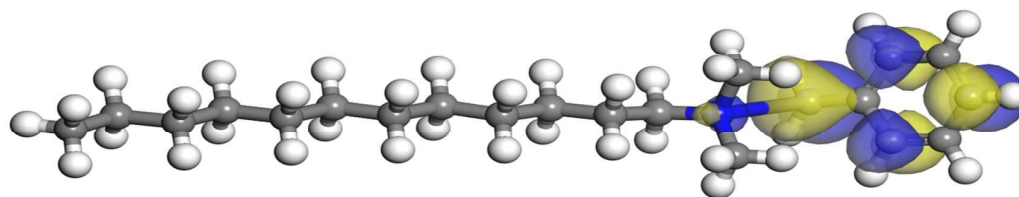


Fig.11 (d): LUMO of dodecyl dimethyl benzyl ammonium bromide (DDBAB) inhibitor

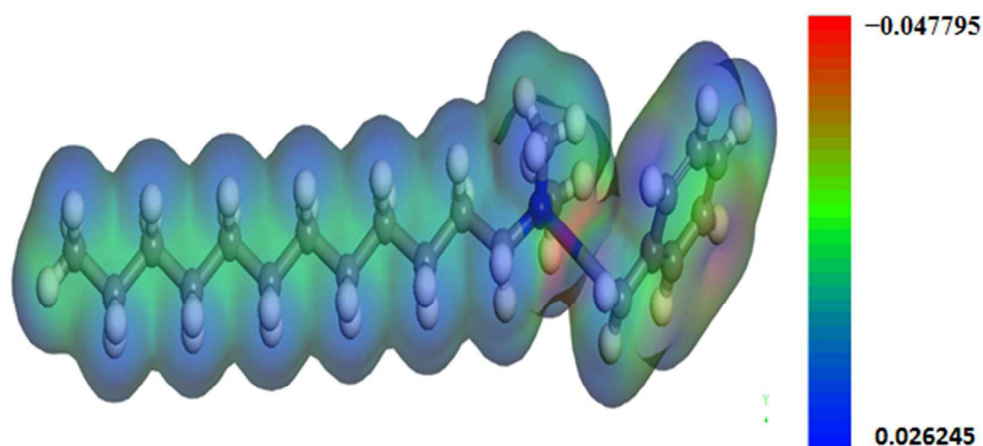


Fig.12. The molecular electrostatic potential of optimized structure of the DDBAB inhibitor.

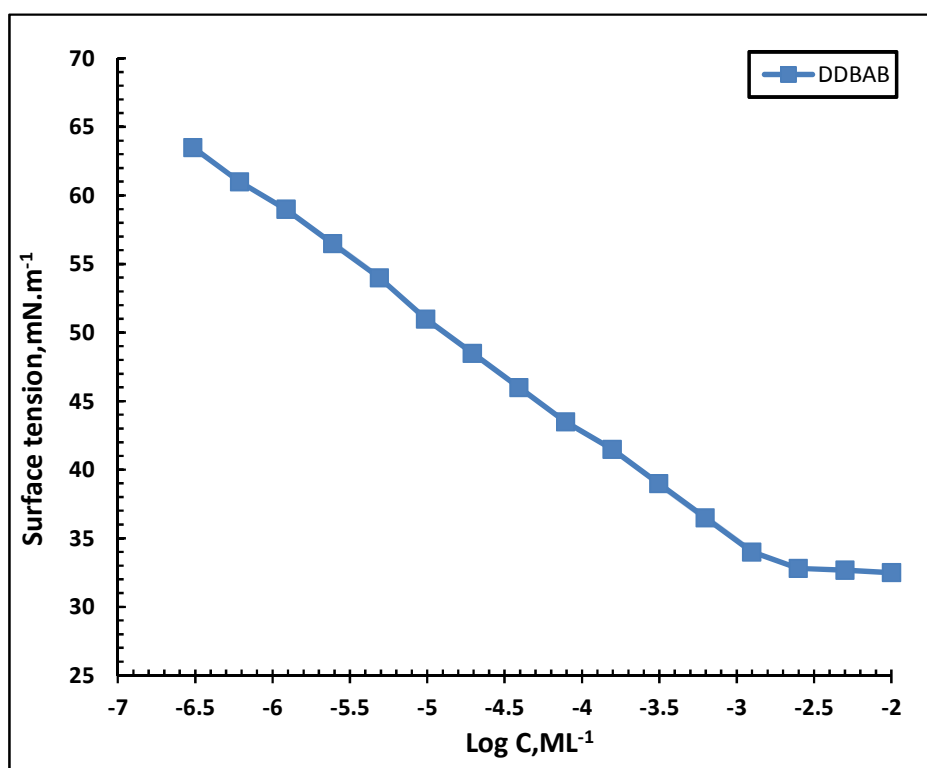


Fig. 13: *surface tension vs. -Log concentration* of the dodecyl dimethyl benzyl ammonium bromide (DDBAB)

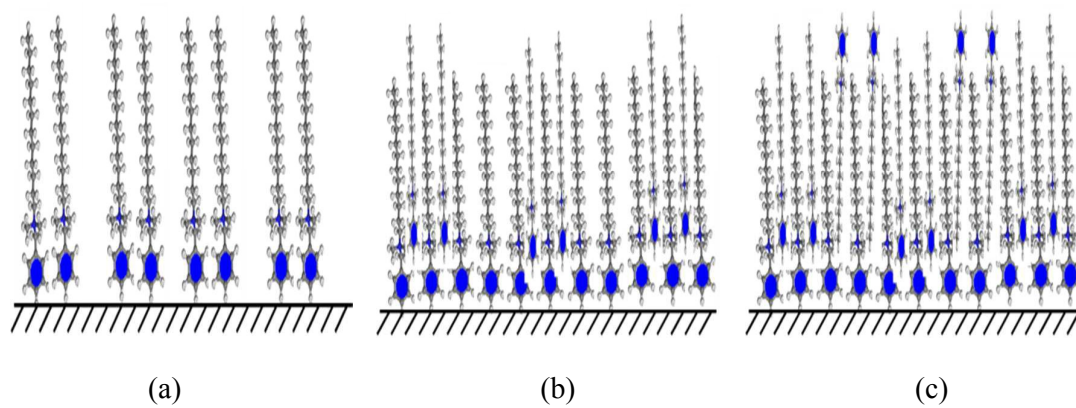


Fig. 14: Schematic representation for the mode of adsorption of (DDBAB) cationic surfactant molecules on carbon steel surface immersed in 8% molar sulfamic acid (a) low concentration, (b) moderate concentration and (c) high concentration.

Table 1. Data obtained from weight loss measurements for X-70 type carbon steel immersed in 8 % sulfamic acid solution in the absence and presence of various concentrations of dodecyl dimethyl benzyl ammonium bromide.

Inhibitor dose, ppm	corrosion rate, mpy	Degree of surface coverage (θ)	Percentage inhibition efficiency, η_w (%)
0	6.0	--	--
30	2.12	0.648	64.8
60	1.64	0.726	72.6
90	1.02	0.832	83.2
120	0.05	0.914	91.4
150	0.46	0.920	92.0

Table 2. Estimation of the equilibrium adsorption constant (K_{ads}) and the free energy of adsorption ΔG_{ads}° of the inhibitor (DDBAB) molecules on surface carbon steel immersed in 8% sulfamic acid solution

Property	Value
K_{ads} (M^{-1})	17739.93
ΔG_{ads}° ($kJ\ mol^{-1}$)	-34.19

Table 3: Electrochemical kinetic parameters obtained from potentiodynamic polarization measurements of X-70 type carbon steel immersed in 8 % sulfamic acid solution in the absence and presence of various concentrations of dodecyl dimethyl benzyl ammonium bromide.

Inhibitor dose, (ppm)	$E_{corr.}$, mV(vs. SCE)	$I_{corr.}$, mAcm ⁻²	β_c , mVdec ⁻¹	β_a , mVdec ⁻¹	R_p , kΩ cm ²	θ	η_p %
8 % Sulfamic acid Solution (blank)	- 518	0.493	144.2	102.5	0.139	--	--
30 ppm	- 536	0.194	142.5	98.4	0.376	0.636	63.6
60 ppm	- 543	0.140	124.3	94.5	0.480	0.714	71.4
90 ppm	- 552	0.103	126.8	92.1	0.731	0.812	81.2
120 ppm	- 564	0.056	128.6	96.3	1.22	0.886	88.6
150 ppm	-568	0.044	122.4	92.6	1.56	0.911	91.1

Table 4: Electrochemical parameters of impedance for X-70 type carbon steel immersed in 8 % sulfamic acid solution in the absence and presence of various concentrations of dodecyl dimethyl benzyl ammonium bromide.

Conc. (ppm)	R_s , (Ω cm ²)	C_f , (μF.cm ²)	n_1	R_f , (Ω cm ²)	C_{dl} , (μF.cm ²)	n_2	R_{ct} , (Ω cm ²)	η_I (%)
blank	4.7	---	0.94	---	22.3	---	85.6	----
30 ppm	5.32	9.8	0.92	19.5	19.5	0.89	230.1	62.8
60 ppm	6.75	7.3	0.88	22.3	16.8	0.87	588.2	85.4
90 ppm	5.55	5.4	0.86	27.8	16.6	0.86	826.3	89.6
120 ppm	5.97	4.6	0.85	33.1	13.4	0.83	1114.8	92.3
150 ppm	6.58	3.9	0.84	34.7	11.1	0.79	1372.4	93.7

Table 5: The calculated quantum chemical parameters obtained from DMOL³ calculations

Inhibitor name	E_{HOMO} (eV)	E_{LUMO} (eV)	ΔE (eV)	D (Debye)	I (eV)	A (eV)	X (eV)	π (eV)	η (eV)	σ (eV ⁻¹)	ω	ΔN
DDBAB	-3.461	-2.255	1.206	1.0466	3.461	2.255	2.858	-2.858	0.603	1.6584	6.773	3.4345

Table 6: Surface activity and thermodynamics properties of dodecyl dimethyl benzyl ammonium bromide (DDBAB) at 25 °C

Compound	CMC (mM/L)	π_{CMC} (mN/m)	γ_{CMC} (mN/m)	$\delta\gamma/\partial \log C$	$\Gamma_{max} \times 10^{10}$ (mol/cm ²)	A_{min} (Å ²)	pC ₂₀ (M/L)	ΔG_{mic}^o (kJ mol ⁻¹)	ΔG_{ads}^o (kJ mol ⁻¹)
DDBAB	1.78	39.3	33	-8.2227	1.66	100.053	-5.1	-15.69	-18.06